Novel approaches to estimating turbulent kinetic energy dissipation rate from low and moderate resolution velocity fluctuation time series

Marta Wacławczyk[1], Yong-Feng Ma[1], Jacek M. Kopeć[1,2], and Szymon P. Malinowski[1]

[1]Institute of Geophysics, Faculty of Physics, University of Warsaw, Warsaw, Poland
[2]Interdisciplinary Centre of Mathematical and Numerical Modelling, University of Warsaw, Warsaw, Poland

Correspondence to: marta.waclawczyk@igf.fuw.edu.pl

Abstract. In this paper we propose two approaches to estimating the kinetic energy dissipation rate, based on the zero-crossing method by Sreenivasan et al. [*J. Fluid Mech.*, **137**, 1983]. The original formulation requires a fine resolution of the measured signal, down to the smallest dissipative scales. However, due to finite sampling frequency, as well as measurement errors, velocity time series obtained from airborne experiments are characterized by the presence of effective spectral cut-offs. In

5 contrast to the original formulation the new approaches are suitable for use with signals originating from such experiments. The fittingness of the new approaches is tested using measurement data obtained during the Physics of Stratocumulus Top (POST) airborne research campaign.

1 Introduction

Despite the fact that turbulence is one of the key physical mechanisms responsible for many atmospheric phenomena, informa-

10 tion on Turbulent Kinetic Energy (TKE) dissipation rate ϵ based on in-situ airborne measurements is scarce. Research aircraft are often not equipped to measure wind fluctuations with spatial resolution better than few tens of meters (Wendisch and Brenguier , 2013). Due to various problems related to e.g. inhomogeneity of turbulence along the aircraft track and/or artifacts related to inevitable aerodynamic problems (Khelif et al., 1999; Kalgorios and Wang, 2002; Mallaun et al., 2015), estimates of ϵ at such low resolutions using power spectral density or structure functions are complex and far from being standardised (e.g.

15 compare procedures in Strauss et al. (2015), Jen-La Plante et al. (2016)). The question arises: can we do any better? Or at least can we introduce alternative methods to increase robustness of ϵ retrievals?

In the literature, there exist several different methods to estimate ϵ using the measured velocity signal as a starting point. One of them is the zero- or threshold-crossing method (Sreenivasan et al., 1983) which, instead of calculating the energy spectrum or velocity structure functions, requires counting of the signal zero- or threshold crossing events are, see Fig. 1a. Their mean

20 number per unit length is related to the turbulent kinetic energy dissipation rate. The zero-crossing method is based on a direct relation between ϵ and the root mean square of the velocity derivative $\langle (\partial u/\partial t)^2 \rangle$ (Pope, 2000), hence, the measured signal should be resolved down to the smallest scales. However, this is not achievable in the case of the moderate-resolution flight measurements, where the sampling frequency is typically $2-3$ orders of magnitude smaller than the frequency corresponding

to the Kolmogorov scales. As a result, the number of zero-crossings per unit length N_L for such signal is much smaller than the one corresponding to a high resolution velocity signal where turbulence intensity is the same.

Interestingly, Kopeć et al. (2016) have shown, that the dissipation rates estimated from such N_L using very low resolution signals, although underestimated, were proportional to ϵ calculated using structure functions scaling in the inertial range. In the follow up analyses we found that this is also the case for moderate-resolution airborne data from different sources. This led us to a question whether it would be possible to modify the zero-crossing method such that it can also be applied to moderate- or low-resolution measurements whilst mitigating the observed underestimation at the same time. In this work we propose two possible modifications of the zero-crossing method. The first one is based on a successive filtering of a velocity signal and inertial-range arguments. In the second approach we use an analytical model for the unresolved part of the spectrum and calculate a correcting factor to N_L, such that the standard relation between ϵ and N_L can be used.

The new approaches are tested on velocity signals obtained during the Physics of Stratocumulus Top (POST) research campaign, which was designed to investigate the marine stratocumulus clouds and the details of vertical structure of stratocumlus-topped boundary layer (STBL) (Gerber et al., 2013; Malinowski et al., 2013). The observed winds were measured using the CIRPAS Twin-Otter research aircraft with sampling frequency $f_s = 40Hz$, which corresponds to the resolution $1.375m$ for the speed of the aircraft $U = 55m/s$. The frequency f_s is placed in the inertial range of the power spectral density (PSD) of the measured signal.

The present paper is structured as follows. In section 2 we review existing methods to estimate dissipation rate of the turbulent kinetic energy. Next, in Section 3 we propose the two modifications of the zero-crossing method. They are applied to a single signal from flight 13 and discussed in detail in Section 4. Next, in Section 5 we apply the procedures to several data sets from flights 10 and 13 to show that the results of new approaches compare favourably with those obtained from standard power-spectrum and structure function methods. This is followed by Conclusions where the advantages of the new proposals and perspectives for further study are discussed.

2 State of the art

The need to estimate the turbulent kinetic energy dissipation rate ϵ as well as variety of available data resulted in formulating a number of estimation methods. Two of the most commonly used approaches are the frequency spectrum and the structure-function approach. Both are based on the inertial-range arguments, which follow from the Kolmogorov's second similarity hypothesis, hence, they are also called "indirect methods" (Albertson et al., 1997). In the homogeneous and isotropic turbulence the one-dimensional longitudinal and transverse wavenumber spectra in the inertial range are given by (Pope, 2000):

$$E_{11}(k_1) = C_1\epsilon^{2/3}k_1^{-5/3}, \quad E_{22}(k_1) = C_1'\epsilon^{2/3}k_1^{-5/3}. \tag{1}$$

Here k_1 is the longitudinal component of the wavenumber vector $\mathbf{k}$, $C_1 \approx 0.49$ and $C_1' \approx 0.65$. E_{11} is related to the energy-spectrum function $E(k)$:

$$E_{11}(k_1) = \int\limits_{k_1}^{\infty} \frac{E(k)}{k} \left(1 - \frac{k_1^2}{k^2}\right) dk. \tag{2}$$

As discussed in Pope (2000) experimental data confirm Eqs. (1) within 20% of the predicted values of C_1 and C_1' over two decades of wavenumbers. The energy-spectrum function in the whole wavenumber range can be approximated by the formula (Pope, 2000):

$$E(k) = C\epsilon^{2/3}k^{-5/3}f_L(kL)f_\eta(k\eta), \tag{3}$$

here $C \approx 1.5$ as supported by experimental data, f_L and f_η are non-dimensional functions, which specify the shape of energy-spectrum in, respectively, the energy-containing and the dissipation range. L denotes the length scale of large eddies and $\eta = (\nu^3/\epsilon)^{1/4}$ is the Kolmogorov length scale connected with the dissipative scales. The function f_L tends to unity for large kL whereas f_η tends to unity for small $k\eta$, such that in the inertial range the formula $E(k) = C\epsilon^{2/3}k^{-5/3}$ is recovered.

Within the validity of the Taylor's hypothesis (1) can be converted to the frequency spectra, where $k = (2\pi f)/U$ and U is the mean velocity of the aircraft. In order to estimate the dissipation rate from the atmospheric turbulence measurements, several assumptions should be taken. Most importantly, one assumes that the turbulence is homogeneous and isotropic and that the inertial range scaling Eqs. (1) holds. Then, frequency spectrum of the longitudinal velocity component reads (e.g., Oncley et al., 1996; Siebert et al., 2006):

$$S(f) = \alpha \left(\frac{U}{2\pi}\right)^{2/3} \epsilon^{2/3} f^{-5/3}, \tag{4}$$

here $\alpha \approx 0.5$. With this, the turbulent kinetic energy dissipation rate can be estimated from the PSD of the measured signal.

Alternatively, one can consider the n-th order longitudinal structure functions $D_n = \langle (u_L(x+r,t) - u_L(x,t))^n \rangle$, here u_L is the longitudinal component of velocity. In the inertial subrange, the second and third-order structure functions are related to the dissipation rate ϵ by the formulas (Pope, 2000):

$$D_2(r) = C_2\epsilon^{2/3}r^{2/3}, \quad D_3(r) = -\frac{4}{5}\epsilon r. \tag{5}$$

Experimental results of Saddoughi and Veeravalli (1994) indicate that $C_2 \approx 2.$ with an accuracy of $\pm 15\%$.

Another method, also based on the formula (3) is the velocity variance method (Fairall et al., 1980; Bouniol et al., 2004; O'Connor et al., 2010). Let us consider a stationary signal $u(t)$. The variance of this signal $\langle u^2(t) \rangle = u'^2$ is equal to the integral of the power spectral density $S(f)$ over the frequency space.

Let us now filter the signal $u(t)$ with a band-pass filter with cut-off numbers $[f_{low}, f_{up}]$ in the frequency space. We obtain a signal $u_f(t)$ with the variance

$$u_f'^2 = \int\limits_{f_{low}}^{f_{up}} S(f) df. \tag{6}$$

The above formula represents the portion of kinetic energy of $u(t)$ contained in the frequencies between f_{low} and f_{up}. If we introduce Eq. (3) for $S(f)$ into (6) and integrate we finally obtain the following formula for the dissipation rate:

$$\epsilon = \left[\frac{2(2\pi)^{2/3} u_f'^2}{3\alpha U^{2/3}(f_{low}^{-2/3} - f_{up}^{-2/3})} \right]^{3/2}.\tag{7}$$

Yet another method, also used in the atmospheric turbulence analysis (Sreenivasan et al., 1983; Poggi and Katul, 2009, 2010;

5   Wilson, 1995; Yee et al., 1995), is based on the number of zero- or level-crossings of the measured velocity signal. It dates back to the early work of Rice (1945) who considered a stochastic processes q and its derivative with respect to time $\partial q/\partial t$. He then assumed that these two processes have Gaussian statistics and are independent. The formulation of this method results from investigating how frequently the signal crosses the level zero $q(t) = 0$, see Fig. 1a. Working under those assumptions Rice (1945) showed that the number of crossings of the zero level per unit time is:

10 $$N^2 = \frac{\langle (\partial q/\partial t)^2 \rangle}{4\pi^2 \langle q^2 \rangle}.\tag{8}$$

As $\langle (\partial q/\partial t)^2 \rangle$ is proportional to the dissipation rate of the kinetic energy, the zero-crossing method can be used to estimate this quantity. As it was argued by Sreenivasan et al. (1983), Eq. (8) holds also with less restricted assumptions, with only q having Gaussian statistics and, moreover, even for strongly non-Gaussian velocity signals the number of zero-crossings was close to the theoretical value (8). For a spatially varying signal, Eq. (8) can be expressed as follows, using the characteristic

15 wavenumber k_c (He and Yuan, 2001):

$$k_c = \sqrt{\frac{\int_0^\infty k^2 E_{11} \mathrm{d}k}{\int_0^\infty E_{11} \mathrm{d}k}}.\tag{9}$$

The characteristic wavelength is equal to $\lambda_c = 2\pi/k_c$. Hence, the mean number of crossings (up- and downcrossings) per unit length N_L, with, on average, two crossing per λ_c is

$$N_L = \frac{2}{\lambda_c} = \frac{1}{\pi} k_c.\tag{10}$$

20 We will now introduce the two-point correlation of velocity $R_{11}(r_1 \mathbf{e}_1) = \langle u_1(\mathbf{x}) u_1(\mathbf{x} + r_1 \mathbf{e}_1) \rangle$. R_{11} and its derivatives can be written in terms of the inverse Fourier transform of E_{11} (Pope, 2000):

$$R_{11}(r_1 \mathbf{e}_1) = \int_0^\infty E_{11}(k_1) \mathrm{e}^{ikr_1} \mathrm{d}k_1, \quad R_{11}''(r_1 \mathbf{e}_1) = -\int E_{11}(k_1) k_1^2 \mathrm{e}^{ik_1 r_1} \mathrm{d}k_1.\tag{11}$$

Using those relationships we can rewrite Eq. (9) in the following manner:

$$k_c = \sqrt{\frac{\int_0^\infty k_1^2 E_{11}(k_1) \mathrm{d}k_1}{\int_0^\infty E_{11}(k_1) \mathrm{d}k_1}} = \sqrt{\frac{-R_{11}''(0)}{R_{11}(0)}}.\tag{12}$$

25 On the other hand, $R_{11}''(0)$ and $R_{11}(0)$ define the Taylor longitudinal microscale λ_f (or the Taylor transverse microscale $\lambda_g = \lambda_f/\sqrt{2}$ - if we consider the transverse velocity correlations):

$$\lambda_f = \left(-\frac{1}{2} \frac{R_{11}''(0)}{R_{11}(0)} \right)^{-1/2}.\tag{13}$$

Hence, Eq. 10 implies that the number of crossings per unit length is related to the longitudinal Taylor's microscale λ_f through

$$\lambda_f = \frac{\sqrt{2}}{\pi}\frac{1}{N_L} \quad\Longrightarrow\quad \frac{1}{\lambda_f^2} = \frac{1}{2}\pi^2 N_L^2. \tag{14}$$

A relation between dissipation and the Taylor microscales reads (Pope, 2000)

$$\epsilon = \frac{15\nu u'^2}{\lambda_g^2} = \frac{30\nu u'^2}{\lambda_f^2}. \tag{15}$$

Hence, finally, substituting (14) into (15) we obtain (Poggi and Katul, 2010)

$$\epsilon = 15\pi^2\nu u'^2 N_L^2. \tag{16}$$

3 New proposals to estimate dissipation rate from a velocity signal with a truncated high-frequency part of the energy spectrum

Based on Eq. (9) and (10) it is clear that the number of zero-crossings is related to the dissipation spectra $D_{11}(k) = 2\nu k^2 E_{11}(k)$:

$$\pi^2 u'^2 N_L^2 = \int_0^\infty k^2 E_{11}\mathrm{d}k. \tag{17}$$

Figure 1b presents the profile of $D(k) = 2\nu k^2 E(k)$ where $E(k)$ is described by the model spectrum (3) with $f_\eta = \exp(-\beta k\eta)$ (Pope, 2000), here $\beta = 2.1$ and $\eta = 2mm$. It is clear that the large wavenumber (small scale) part of the spectrum has the most significant impact on the resulting value of N_L.

At the same time the data available from the POST measurements, where the sampling frequency was restricted to $f_s = 40Hz$, can only account for a small part of the total dissipation spectrum (shaded regions in Fig. 1). If one was to use this zero-crossing method (Eq. 16) in order to estimate ϵ it is clear that the measured number of signal zero-crossings would lead to significant underestimation of the spectrum integral as compared to the full spectrum measurements down to the very small scales. We would like to propose reformulation of the original zero-crossing method in order to estimate the dissipation rate from the number of signal zero-crossings based on a restricted range of k-values available from the airborne measurements. Two proposals for such procedures are given further in the article.

3.1 Method based on successive filtering of a signal

Let us consider a signal $u_1(t)$ resolved in a certain range of frequencies $f_0 < f < f_1$. Converting the wavenumber spectrum to the frequency spectrum we obtain from Eq. (17) the following relation for the number of signal-crossings per unit time

$$u_1'^2 N_1^2 = 4\int_{f_0}^{f_1} f^2 S(f)\mathrm{d}f. \tag{18}$$
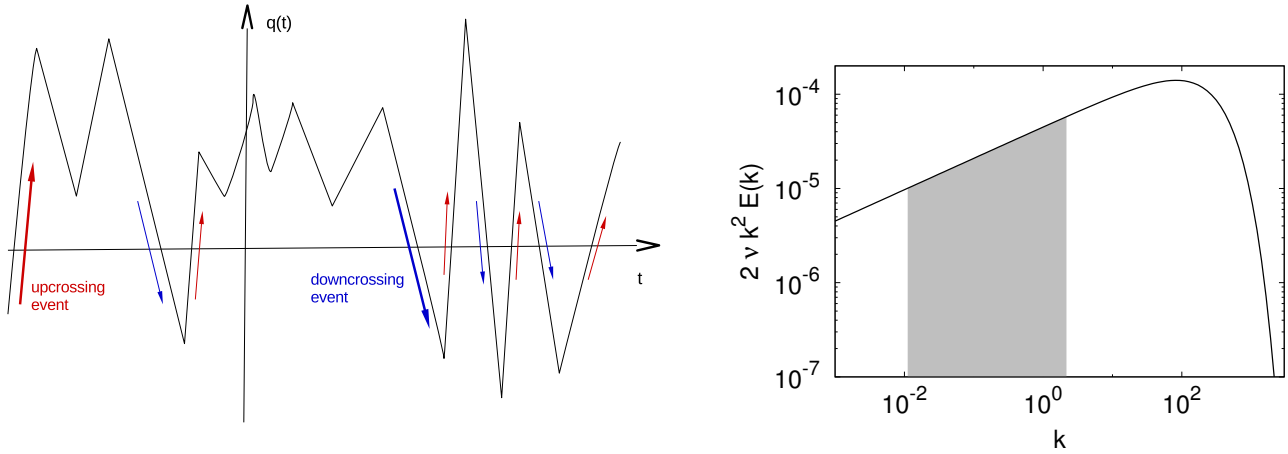
Figure 1. a) A signal $q(t)$ crossing the level $q = 0$. b) Dissipation spectra: the range of k-numbers covered by the POST measurements is denoted by the colour shading.

Similarly as in the velocity variance method described in Section 2, let us now filter the signal using a low-pass filter characterized by a different cut-off frequency $f_2 < f_1$. In such a case we obtain a different signal $u_2(t)$ with a reduced number of zero-crossings $N_2 < N_1$:

$$u_2^{'2} N_2^2 = 4 \int_{f_0}^{f_2} f^2 S(f) \mathrm{d}f. \tag{19}$$

5   If we subtract (19) from (18) we obtain

$$(u_1^{'2} N_1^2 - u_2^{'2} N_2^2) = 4 \int_{f_2}^{f_1} f^2 S(f) \mathrm{d}f. \tag{20}$$

In the inertial range $S(f)$ is described by Eq. (4), hence, if both f_1 and f_2 belong to the inertial range

$$(u_1^{'2} N_1^2 - u_2^{'2} N_2^2) = 4\alpha \left(\frac{U}{2\pi}\right)^{2/3} \epsilon^{2/3} \int_{f_2}^{f_1} f^{1/3} \mathrm{d}f = 3\alpha \left(\frac{U}{2\pi}\right)^{2/3} \epsilon^{2/3} \left(f_1^{4/3} - f_2^{4/3}\right). \tag{21}$$

If we proceed further and filter the signal using a series of cut-off frequencies $f_i < f_2$, we can estimate ϵ form Eq. (21) using a
10   linear least squares fitting method.

3.2   Method based on recovering the missing part of the spectrum

In this method we attempt to account for the impact of the missing part of the dissipation spectrum by introducing a correcting factor to the number of zero-crossings per unit length N_L. The number of crossings per unit length is calculated from the

measured signal where the fine-scale fluctuations having the highest wavenumber k_{cut} will be denoted by N_{cut} and the variance of this signal will be denoted by u'^2_{cut}. From Eq. (17) it follows that N_{cut} is related to N_L by the formula

$$u'^2 N_L^2 = u'^2_{cut} N_{cut}^2 \frac{\int_0^\infty k_1^2 E_{11} \mathrm{d}k_1}{\int_0^{k_{cut}} k_1^2 E_{11} \mathrm{d}k_1} = u'^2_{cut} N_{cut}^2 \left(1 + \frac{\int_{k_{cut}}^\infty k_1^2 E_{11} \mathrm{d}k_1}{\int_0^{k_{cut}} k_1^2 E_{11} \mathrm{d}k_1} \right). \tag{22}$$

We then assume a certain form of the energy spectrum (3) with $f_\eta = \mathrm{e}^{-\beta k \eta}$, here $\beta = 2.1$ (Pope, 2000) and $f_L = 1$, as the largest scales do not contribute much to the final value of the dissipation rate. With this, the energy spectrum reads

$$E(k) = C \epsilon^{2/3} k^{-5/3} \mathrm{e}^{-\beta k \eta}, \tag{23}$$

here $C = 1.5$. The integral of the dissipation spectrum $2\nu k^2 E(k)$ should be equal to ϵ, which implies that $\beta = 2.1$. Hence, rather than being an empirical constant, the value of β in Eq. (23) is fixed by theoretical constrains. The corresponding one-dimensional spectrum E_{11} can be calculated from Eq. (2)

$$E_{11}(k_1) = C \epsilon^{2/3} \int_{k_1}^\infty k^{-8/3} \mathrm{e}^{-\beta k \eta} \left(1 - \frac{k_1^2}{k^2} \right) \mathrm{d}k. \tag{24}$$

As a result of introducing Eq. (24) into Eq. (22) and some additional rearrangements we obtain

$$u'^2 N_L^2 \approx u'^2_{cut} N_{cut}^2 \left[1 + \frac{\int_{k_{cut}\beta\eta}^\infty k_1^2 \int_{k_1}^\infty k^{-8/3} \mathrm{e}^{-k} \left(1 - \frac{k_1^2}{k^2} \right) \mathrm{d}k \mathrm{d}k_1}{\int_0^{k_{cut}\beta\eta} k_1^2 \int_{k_1}^\infty k^{-8/3} \mathrm{e}^{-k} \left(1 - \frac{k_1^2}{k^2} \right) \mathrm{d}k \mathrm{d}k_1} \right] = u'^2_{cut} N_{cut}^2 \mathcal{C_F}, \tag{25}$$

here $\mathcal{C_F}$ is the correcting factor

$$\mathcal{C_F} = 1 + \frac{\int_{k_{cut}\beta\eta}^\infty k_1^2 \int_{k_1}^\infty k^{-8/3} \mathrm{e}^{-k} \left(1 - \frac{k_1^2}{k^2} \right) \mathrm{d}k \mathrm{d}k_1}{\int_0^{k_{cut}\beta\eta} k_1^2 \int_{k_1}^\infty k^{-8/3} \mathrm{e}^{-k} \left(1 - \frac{k_1^2}{k^2} \right) \mathrm{d}k \mathrm{d}k_1}. \tag{26}$$

The value of ϵ can be calculated numerically using an iterative procedure.

As a starting point for this procedure, a first guess for the Kolmogorov length $\eta = (\nu^3/\epsilon)^{1/4}$ should be given. With this, we calculate the correcting factor $\mathcal{C_F}$ from Eq. (26) and next, from Eq. (16) the value of dissipation can be estimated as

$$\epsilon = 15 \pi^2 \nu u'^2 N_{cut}^2 \mathcal{C_F}. \tag{27}$$

We start the next iteration by calculating again the Kolmogorov length $\eta = (\nu^3/\epsilon)^{1/4}$, the corrected value of $\mathcal{C_F}$ from Eq. (26) and the new value of ϵ from Eq. (27). After several iterations the procedure converges to the final values of the dissipation rate and Kolmogorov's length η with an error defined by a prescribed norm $\Delta\eta = |\eta^{n+1} - \eta^n| \le d_\eta$. The successive steps are summarized in a form of algorithm 3.2.

It should be noted that in this approach we do not have the empirical inertial-range constant C, and we calculate the dissipation rate directly from the formula with viscosity (27), as in the original zero-crossing method see Eq. (16) and Poggi and Katul (2010).

Algorithm 1 Procedure of iterative ϵ determination based on missing spectrum part recovery

---

$\epsilon \leftarrow 15\pi^2\nu u'^2 N_{cut}^2$

$\eta \leftarrow (\nu^3/\epsilon)^{1/4}$

$\Delta\eta \leftarrow 100d_\eta$

while $\Delta\eta > d_\eta$ **do**

    Use Eq. (26) to calculate $\mathcal{C_F}$

    $\epsilon \leftarrow 15\pi^2\nu u'^2 N_{cut}^2 \mathcal{C_F}$

    $\Delta\eta \leftarrow |\eta - (\nu^3/\epsilon)^{1/4}|$

    $\eta \leftarrow (\nu^3/\epsilon)^{1/4}$

end while

---

4 In depth analysis of the proposed methods' behaviour

4.1 Method based on the number of zero-crossings of successively filtered signal

In order to present the more detailed properties of the procedure we used velocity signal from one of the horizontal flight segments that took place within the turbulent atmospheric boundary layer. This segment was a part of flight 13 of the POST airborne research campaign (Gerber et al., 2013; Malinowski et al., 2013). The data were provided in the East, North, Up (ENU) coordinate system. For further study we have chosen the second (NS) velocity component. The signals sampling frequency was $f_s = 40\,\text{Hz}$ and the duration was $t = 438.75\,\text{s}$. The mean flight velocity U during that time was about $55\,\text{ms}^{-1}$ and the standard deviation $u' = 0.28\text{ms}^{-1}$.

We have estimated the dissipation rate based on the number of zero-crossings, according to the methods outlined in section 3.1. The dissipation rate calculated from the frequency spectrum and the structure function for the whole flight fragment Eqs. (4) and (5) was equal, respectively, $\epsilon_{PSD} = 2.48 \times 10^{-4}\,\text{m}^2\text{s}^{-3}$ and $\epsilon_{SF} = 2.52 \times 10^{-4}\,\text{m}^2\text{s}^{-3}$. These values were obtained from the linear least-squared fit procedure in the range $f = 0.3 - 5\,\text{Hz}$ for the frequency spectrum and $r = 11 - 183\,\text{m}$ for the structure function, see Fig. 2.

Before applying the threshold crossing procedures the signal had to be filtered in order to eliminate errors due to large scale tendencies as well as small scale measurements noise. For this purpose we used the sixth order low-pass Butterworth filter implemented in Matlab (Butterworth, 1930). Figure 3 presents the velocity signal over $t = 50$s before filtering (top graph) and the same signal after filtering with $f_{cut} = 5\,\text{Hz}$ and $f_{cut} = 1\,\text{Hz}$.

The probability density functions (PDF) of the normalised original signal and the filtered signals (Figure 4a) can all be approximated by the normalised Gaussian distribution, hence, the application of the zero-crossing method is justified, also for the filtered signals. It is worth noting that the spectra ($f^2S(f)$, Fig. 4a) display a peak at $f = 10Hz$. This phenomenon has been indicated in the previous analyses of POST (Jen-La Plante et al., 2016) and appears due to measurement errors. We will address this issue further in this paper.
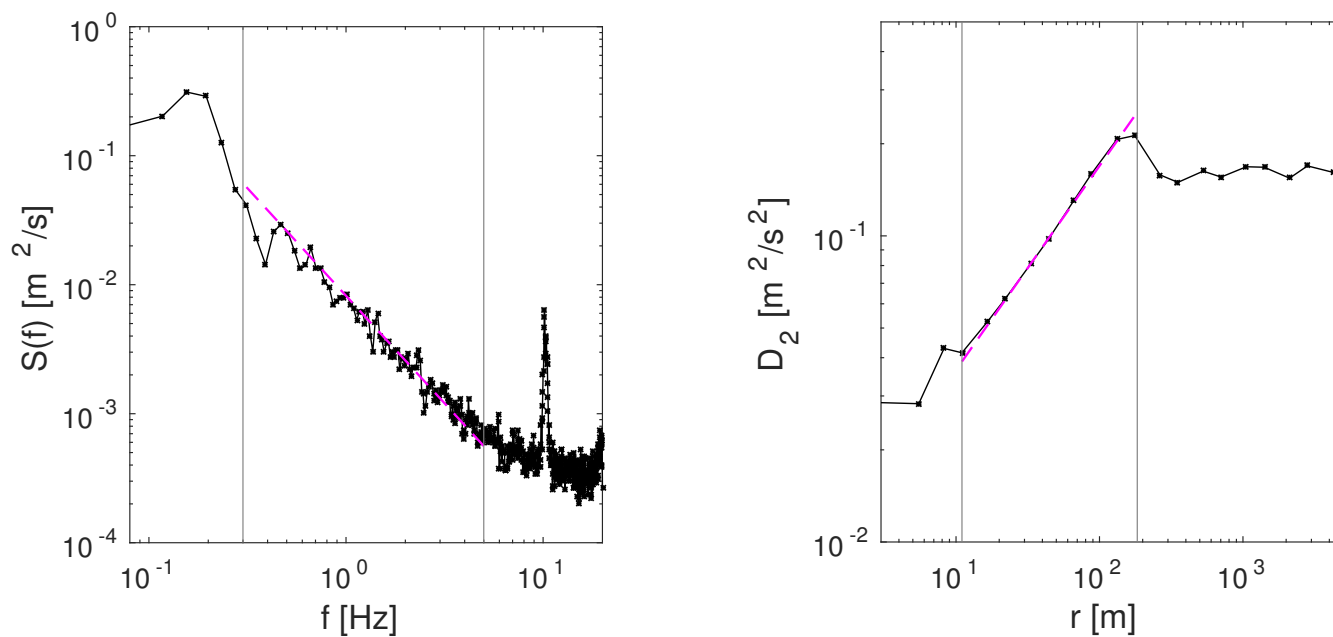
Figure 2. a) Frequency spectrum, b) second order structure function. Polynomial fit is presented as a coloured dashed line.
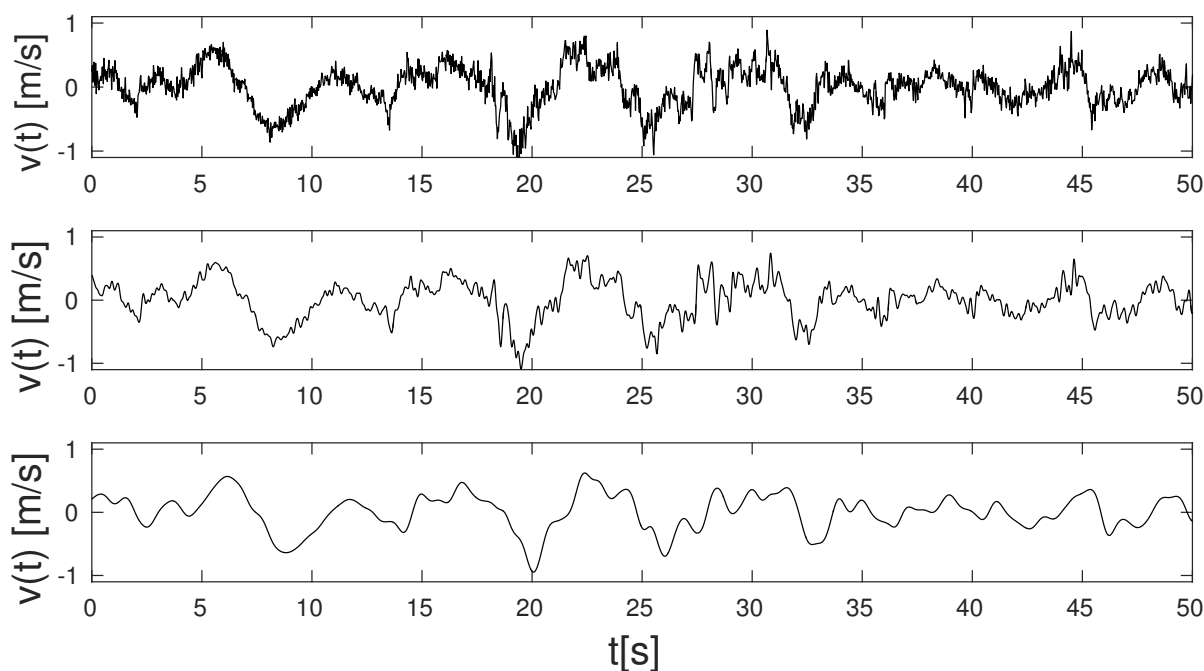
Figure 3. Velocity fluctuations: top graph - unfiltered signal, middle graph - signal filtered with $f_{cut} = 5\,\mathrm{Hz}$, bottom graph - signal filtered with $f_{cut} = 1\,\mathrm{Hz}$.
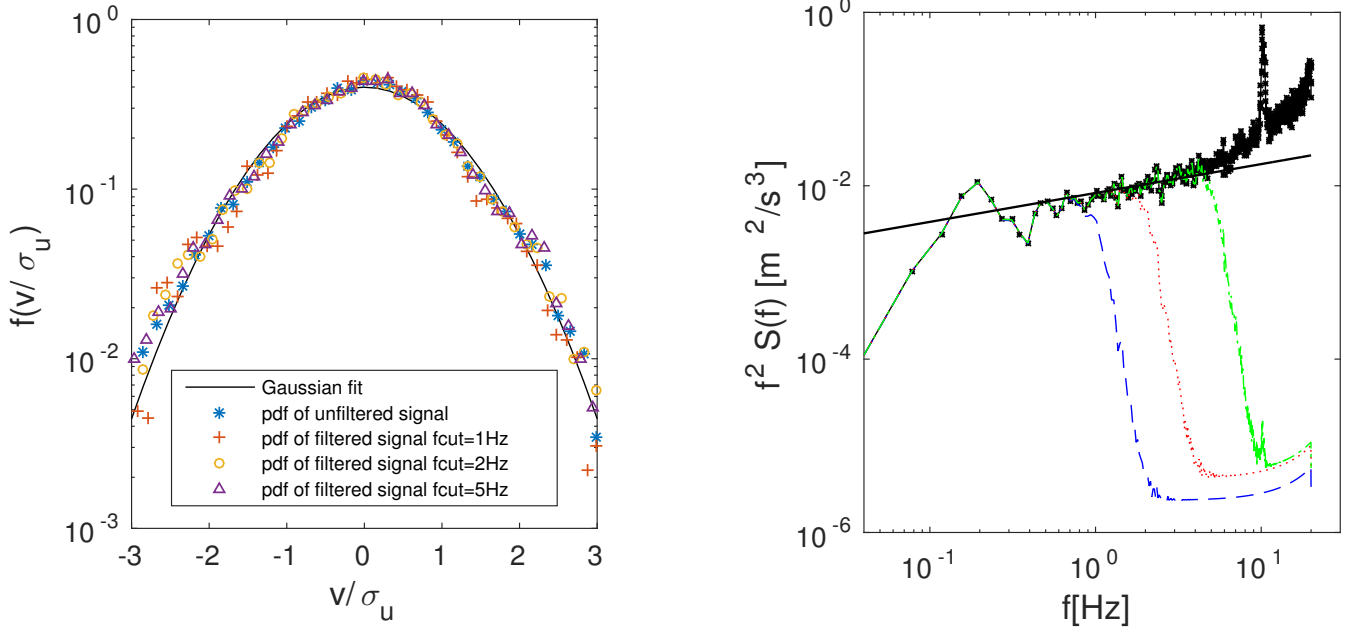
Figure 4. a) PDF's of the normalised unfiltered and filtered signals compared with the normalised Gaussian curve. b) Spectra $f^2 S(f)$ of the unfiltered signal (black line with symbols), signal filtered with $f_{cut} = 5\,\text{Hz}$ (green, solid line), signal filtered with $f_{cut} = 2\,\text{Hz}$ (red dotted line), signal filtered with $f_{cut} = 1\,\text{Hz}$ (blue, dashed line).

In order to use the method based on successive signal filtering we filtered the signal with different values of f_{cut} in the range $f_{cut} = 0.1 - 19\,\text{Hz}$. For each $f_{cut} = f_i$ we calculated the number of zero-crossings N_i based on the filtered signal. The zero-crossing event was detected when the product of two consecutive values of velocity fluctuation $v(t)v(t + \Delta t) < 0$, here $\Delta t = 1/f_s = 0.025\,\text{s}$. First observation is that N_i decreases with decreasing f_i, see Fig. 5a. In order to estimate the value of

5   dissipation rate we used Eq. (21) that was for the convenience of use rewritten as

$$(u_i'^2 N_i^2 - u_1'^2 N_1^2) = 3\alpha \left(\frac{U}{2\pi}\right)^{2/3} \epsilon^{2/3} \left(f_i^{4/3} - f_1^{4/3}\right). \tag{28}$$

Results for $f_1 = 0.3\,\text{Hz}$ and f_i in the range $(0.3\,\text{Hz}, 5\,\text{Hz})$ are presented in Fig. 5b. Using Eq. (28) we have used linear fitting of the differences $u_i'^2 N_i^2 - u_1'^2 N_1^2$ against $f_i^{4/3} - f_1^{4/3}$. The resulting value for the analysed flight section was $\epsilon_{NCF} = 2.54 \times 10^{-4}\,\text{m}^2\text{s}^{-3}$. This value is comparable with the estimations performed using classic methods based on the power spectra and

10   structure functions which resulted respectively in $\epsilon_{PSD} = 2.48 \times 10^{-4}\,\text{m}^2\text{s}^{-3}$ and $\epsilon_{SF} = 2.52 \times 10^{-4}\,\text{m}^2\text{s}^{-3}$.

4.2 Method based on missing spectrum recovery

The same signal was also analysed using the second method proposed in Section 3.2, Eqs. (26,27). In order to simplify numerical implementation of the method we notice that for the assumed form of the spectrum $E(k)$ given in Eq. (23), the formula
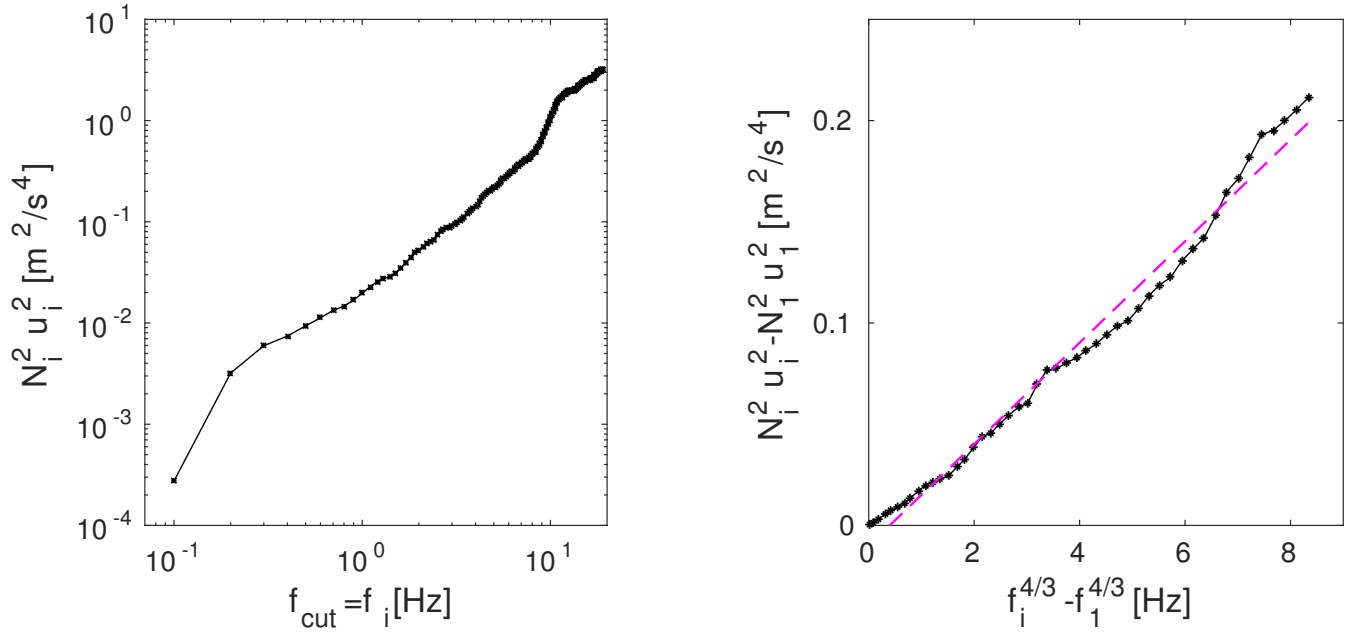
Figure 5. Scaling of $N_i^2 u_i^2$ with filter cut-off f_{cut}. The linear fit from formula (28) is given by the magenda dashed line.

(24) for the one-dimensional spectrum $E_{11}(k_1)$ can be written in terms of the incomplete Γ function as follows

$$E_{11}(k_1) = C\epsilon^{2/3}(\beta\eta)^{5/3}\left[\Gamma(-5/3, k_1\beta\eta) - (\beta\eta)^2 k_1^2\Gamma(-11/3, k_1\beta\eta)\right], \tag{29}$$

here

$$\Gamma(a, x) = \int_x^\infty e^{-t} t^{a-1}\mathrm{d}t. \tag{30}$$

5 The correcting factor (26) in terms of the Γ functions reads

$$\mathcal{C}_{\mathcal{F}} = 1 + \frac{\int_{k_{cut}\beta\eta}^\infty k_1^2\left[\Gamma(-5/3, k_1) - k_1^2\Gamma(-11/3, k_1)\right]\mathrm{d}k_1}{\int_0^{k_{cut}\beta\eta} k_1^2\left[\Gamma(-5/3, k_1) - k_1^2\Gamma(-11/3, k_1)\right]\mathrm{d}k_1}. \tag{31}$$

This is a function of a single argument $(k_{cut}\beta\eta)$. For reference it is plotted in Fig. 6a.

With such preparation we applied the iterative procedure, as described in Section 3.2. In POST experiment the effective cut off frequency was estimated at $f_{cut} = 5\,\mathrm{Hz}$ which corresponds to $k_{cut} = (2\pi f)/U = 0.57\,\mathrm{m}^{-1}$. Using the sixth order

10 Butterworth filter this resulted in $u'^2 N_{cut}^2 = 0.0000719 \cdot 1/s^2$ for this signal. Accordingly we used the algorithm (3.2) with $\nu = 1.5 \cdot 10^{-5}\mathrm{m}^2\mathrm{s}^{-1}$ and $d_\eta = 10^{-6}\mathrm{m}$. We approximated the integrals in Eq. (31) using the trapezoid rule. The results of successive approximations of $\mathcal{C}_{\mathcal{F}}$ and ϵ converge fast to a fixed value, independently of the initial guess of $\epsilon = \epsilon_0$ (Figs. 6a and 6b). The increment $\mathrm{d}k_1$ in Eq. (31) was approximated by $\Delta k_1 = 5 \cdot 10^{-6}\,\mathrm{m}^{-1}$. For such choice we obtained $\epsilon_{NCR} =$
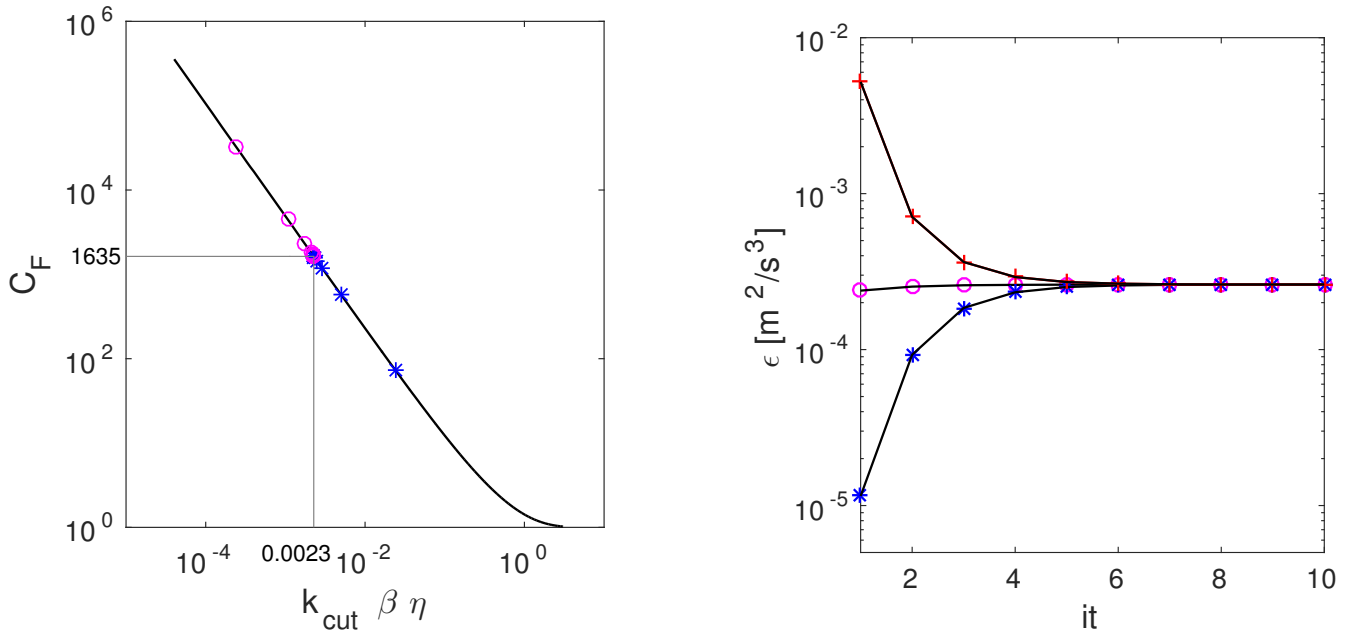
Figure 6. a) Correcting factor (black line), successive values of $\mathcal{C}_{\mathcal{F}}$ obtained during the iteration procedure: with the initial guess of ϵ, $\epsilon_0 = 25\,\mathrm{m^2 s^{-3}}$ (stars), $\epsilon_0 = 2.5 \cdot 10^{-8}\,\mathrm{m^2 s^{-3}}$ (circles). b) Values of ϵ calculated during the iterative procedure for different initial guesses of ϵ_0.
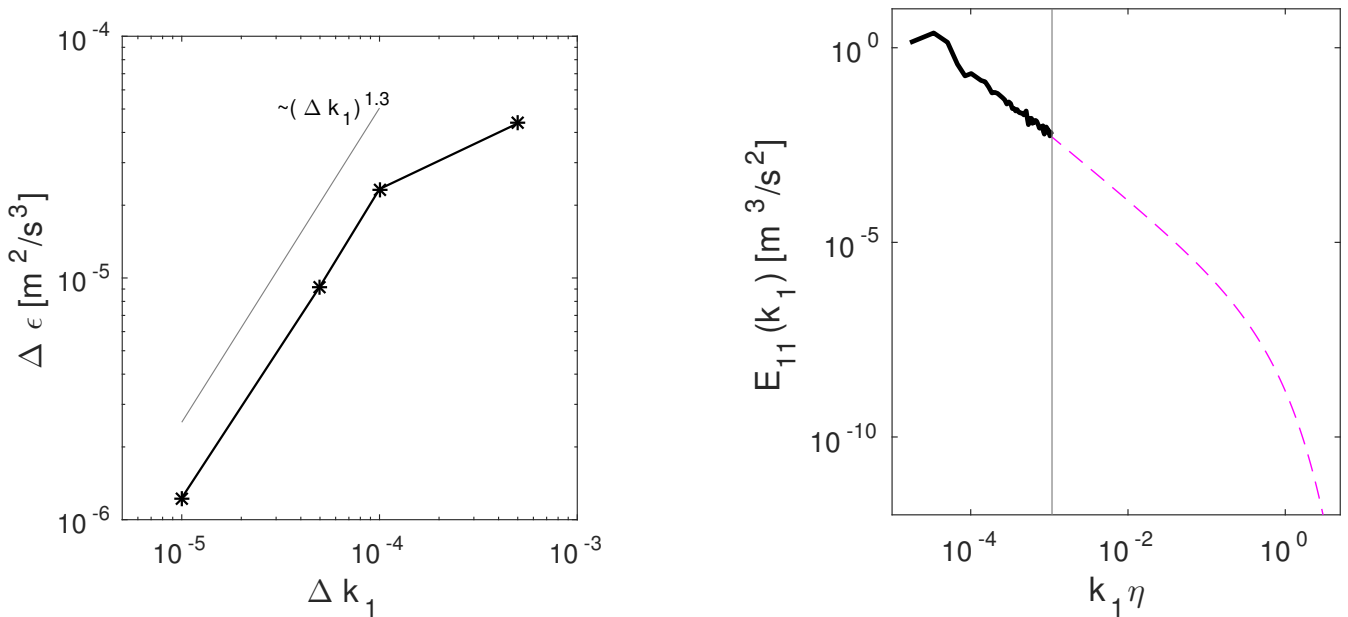
Figure 7. a) a) Error of ϵ as a function of Δk. The reference value is ϵ calculated with $\Delta k = 5 \cdot 10^{-6}\,\mathrm{m^{-1}}$. b) One-dimensional energy spectrum: black solid line: measured part, dashed magenda line: recovered part.

$2.61 \cdot 10^{-4} \, \mathrm{m^2 s^{-3}}$. We used this as a reference value. In order to estimate the numerical accuracy of the proposed algorithm we calculated the error $\Delta \epsilon = |\epsilon - \epsilon_{NCR}|$ for different values of Δk_1, see Fig. 7a. We obtain $\Delta \epsilon \sim \Delta k_1^{1.3}$.

It is worth noting that the proposed method is accounting for a dominant (and not directly measured) part of the spectrum based on the theoretical knowledge about its shape. This knowledge is simply reduced to the form of the correcting factor $\mathcal{C_F}$. Fig. 7b illustrates the relation between the measured and the estimated part of the spectrum for the analysed case.

The result of application of this method $\epsilon_{NCR} = 2.61 \cdot 10^{-4} \, \mathrm{m^2 s^{-3}}$ is comparable with the dissipation rates obtained using other methods, as discussed in Section 3.1, $\epsilon_{PSD} = 2.48 \cdot 10^{-4} \, \mathrm{m^2 s^{-3}}$, $\epsilon_{SF} = 2.52 \cdot 10^{-4} \, \mathrm{m^2 s^{-3}}$ and $\epsilon_{NCF} = 2.54 \cdot 10^{-4} \, \mathrm{m^2 s^{-3}}$. The relative differences between those estimations are less than 5%.

5 Broader overview of the methods' performance

Following the findings presented in the previous section both proposed methods were tested on much larger collection of data. For this purpose we used velocity signals also obtained during the POST research campaign. We have chosen horizontal segments at various levels within the boundary layer from flights $TO10$ and $TO13$. These flights were investigated in detail by Malinowski et al. (2013), due to the fact that they represent two thermodynamically and microphysically different types of stratocumulus topped bondary layer.

The dissipation rates of turbulent kinetic energy estimated from the standard structure function method ϵ_{SF} and dissipation rates estimated from the modified zero-crossing methods ϵ_{NCF} and ϵ_{NCR} introduced in Sections 3.1 and 3.2, respectively, are compared with the results obtained from the power spectra method ϵ_{PSD} in Fig. 8. For flight 10 we obtained the following linear fits and the correlation coefficients r

$$
\begin{aligned}
\epsilon_{SF} &= 0.74 \, \epsilon_{PSD} + 9.1 \cdot 10^{-5}, & r &= 0.997, \\
\epsilon_{NCF} &= 0.88 \, \epsilon_{PSD} + 1.2 \cdot 10^{-5}, & r &= 0.995, \\
\epsilon_{NCR} &= 0.66 \, \epsilon_{PSD} + 7.9 \cdot 10^{-5}, & r &= 0.997,
\end{aligned}
$$

while for flight 13 we have

$$
\begin{aligned}
\epsilon_{SF} &= 0.76 \, \epsilon_{PSD} + 1.4 \cdot 10^{-4}, & r &= 0.956, \\
\epsilon_{NCF} &= 0.75 \, \epsilon_{PSD} + 1.2 \cdot 10^{-4}, & r &= 0.881, \\
\epsilon_{NCR} &= 0.62 \, \epsilon_{PSD} + 1.4 \cdot 10^{-4}, & r &= 0.989.
\end{aligned}
$$

The methods based on the signal zero-crossings give comparable results to those resulting from standard methods. It seems that ϵ_{NCR} is slightly underestimated as compared to the results of the other methods, however it should be noted that while all other methods are based on the inertial-range arguments, in order to obtain ϵ_{NCR} one needs to use viscosity and full spectrum assumptions (resulting from the use of Eq. (27)). Hence, due to different physical arguments we can expect the results to be somewhat different than in case of the previous methods. We believe that the there is a fair consistency in those results because
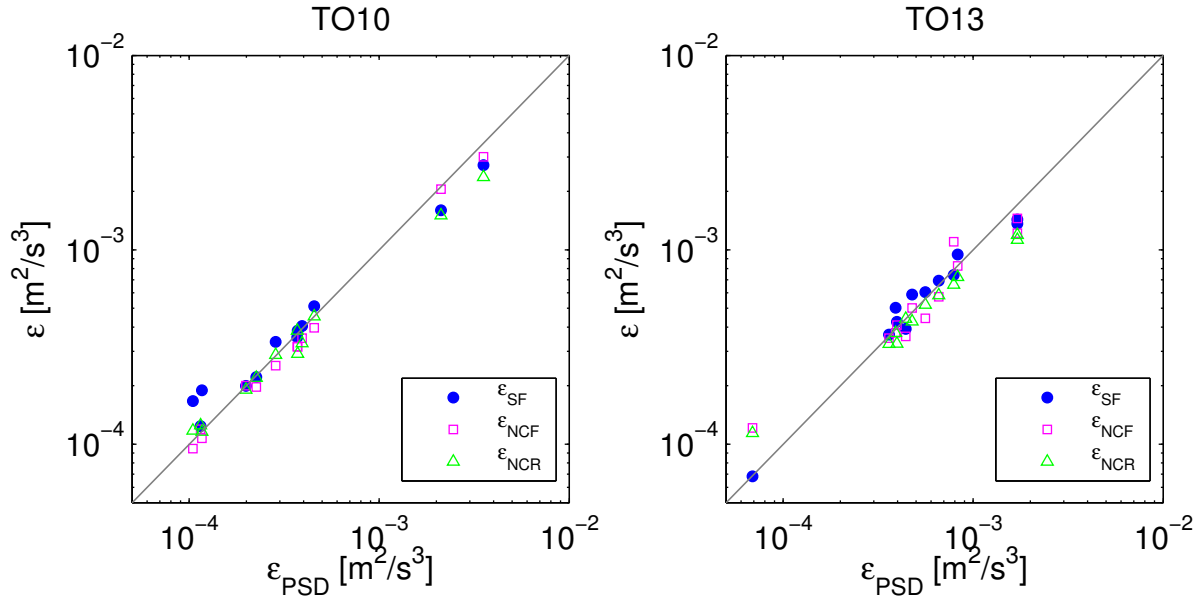
Figure 8. Dissipation rate of the kinetic energy estimated from the structure function method ϵ_{SF}, zero-crossings of successively filtered signals ϵ_{NCF} and zero-crossings of signals with recovered part of the spectrum ϵ_{NCR} as a function of ϵ_{PSD} (from power spectra method). Each point represents an estimate from a single horizontal segment of flight in the atmospheric boundary layer, a) flight 10, b) flight 13.

one should take into account that the standard frequency spectra and structure function methods calculate approximate values of ϵ. Moreover, we have indicated in Section 2 that the constants α and C_2 in Eqs. (4) and (5) are estimated with an accuracy of $\pm 15\%$.

6   Conclusions

5   In the present work we proposed two novel modifications of the zero-crossing method, such that it can be applied to moderate-resolution measurements. Turbulent kinetic energy dissipation rates obtained using the proposed methods were compared to the estimates resulting from the use of the standard power-spectrum and structure function approaches. It is a remarkable testimony to the statistical turbulence theory consistency that those results are in quite good agreement despite using such fundamentally different approaches.

10   From the perspective of practical applications we can think of several possible advantages of the zero-crossing methods. First, the number of signal zero-crossings can be calculated without difficulty and the proposed procedures are easy to implement. Second, it is not necessary to choose any averaging windows, as it is the case for the power-spectrum and structure function methods. Hence, the obtained results will not depend on the width of this window. Finally, we can deal with a situation when the recorded amplitude of certain frequencies is deteriorated due to measurement errors (e.g. as it is seen in Fig. 4b, we have a

15   spurious peak at $f = 10 Hz$), still, the counted number of signal zero-crossings could remain unaffected (see e.g. Fig. 5a, where

no distortion at $f = 10Hz$ is observed). In such cases the zero-crossing method could be advantageous over the power-spectrum and structure-function methods.

There are several perspectives for further work. First, the proposed methods could be tested for a wider range of signals (e.g. from Eulerian measurements within the boundary layer adopting Taylor hypothesis), characterized by different resolutions and obtained under varying atmospheric conditions, to assess the scope of their applicability. Second, as far as the model spectrum is concerned, instead of (23) different forms for the function f_η in Eq. (3) could be tested (see e.g. Chap. 6.5.3 in Pope (2000) or Bershadskii (2016)). In the present study we have chosen the simplest form of f_η, Eq. (23), in order to present the one-dimensional energy spectrum E_{11} in terms of Γ functions, see Eq. (29). However, other forms of spectrum could have potentially significant impact on the results which should be analysed.

7   Code availability

The MATLAB code written for the purpose of this study is available from the authors upon request.

8   Data availability

POST data are available in the open database: https://www.eol.ucar.edu/projects/post/

Acknowledgements.   We acknowledge financial support of the National Science Centre, Poland: MW through the project 2014/15/B/ST8/00180, Y-FM and SPM through the project 2013/08/A/ST10/00291. The POST field campaign was supported by US National Science Foundation through grant ATM-0735121 and by the Polish Ministry of Science and Higher Education through grant 186/W-POST/2008/0.

References

Bershadskii A.: Distributed chaos and inertial ranges in turbulence, arXiv:1609.01617, 2006.

Albertson, J. D., Parlange, M. B., Kiely, G. and Eichinger, W. E.: The average dissipation rate of turbulent kinetic energy in the neutral and unstable atmospheric surface layer, 102, 13423–13432, 1997

5   Bouniol, D., Illingworth, A., and Hogan, R.: Deriving turbulent kinetic energy dissipation rate within clouds using ground based radar, in: Proceedings of ERAD, vol. 281, 2004.

Butterworth S.: On the theory of filter amplifiers, Experimental Wireless and the Wireless Engineer, 7, 536–541, 1930.

Fairall, C., Markson, R., Schacher, G., and Davidson, K.: An aircraft study of turbulence dissipation rate and temperature structure function in the unstable marine atmospheric boundary layer, Boundary-Layer Meteorology, 19, 453–469, 1980.

10   Gerber, H., Frick, G., Malinowski, S. P., Jonsson, H., Khelif, D., and Krueger, S. K.: Entrainment rates and microphysics in POST stratocumulus, Journal of Geophysical Research: Atmospheres, 118, doi:10.1002/jgrd.50878, 2013.

He, W.-Z. and Yuan M.-S.: Statistical Property of Threshold-Crossing for Zero-Mean-Valued, Narrow-Banded Gaussian Processes, Applied Mathematics and Mechanics, 22, 701-710, 2001.

Jen-La Plante, I., Ma, Y., Nurowska, K., Gerber, H., Khelif, D., Karpinska, K., Kopec, M., Kumala, W., and Malinowski, S.: Physics of

15   Stratocumulus Top (POST): turbulence characteristics, Atmospheric Chemistry and Physics, 16, 9711–9725, doi:10.5194/acp-16-9711-2016, 2016.

Kalogiros J. A. and Wang Q.: Calibration of a Radome-Differential GPS System on a Twin Otter Research Aircraft for Turbulence Measurements, J. Atmos. Ocean. Technol., 19, 159–171, 2002, doi: 10.1175/1520-0426(2002)019<0159:COARDG>2.0.CO;2.

Khelif, D., Burns S. P., and Friehe C. A.: Improved Wind Measurements on Research Aircraft, J. Atmos. Ocean. Technol., 16, 860–875,

20   1999.

Kopeć, J.M., Kwiatkowski, K., de Haan, S. and Malinowski, S.P.: Retrieving atmospheric turbulence information from regular commercial aircraft using Mode-S and ADS-B, Atmos. Meas. Tech., 9, 2253-2265, 2016, doi: 10.5194/amt-9-2253-2016.

Malinowski, S.P., Gerber, H., Jen-La Plante, I., Kopec, M.K., Kumala, W., Nurowska, K., Chuang, P.Y., Khelif, D. and Haman, K.E.: Physics of Stratocumulus Top (POST): turbulent mixing across capping inversion, Atmospheric Chemistry and Physics, 13, 12171-12186, 2013,

25   doi: 10.5194/acp-13-12171-2013

Mallaun, C., Giez, A., and Baumann, R.: Calibration of 3-D wind measurements on a single-engine research aircraft, Atmos. Meas. Tech., 8, 3177-3196, doi:10.5194/amt-8-3177-2015, 2015.

O'Connor, E. J., Illingworth, A. J., Brooks, I. M., Westbrook, C. D., Hogan, R. J., Davies, F., and Brooks, B. J.: A method for estimating the turbulent kinetic energy dissipation rate from a vertically pointing Doppler lidar, and independent evaluation from balloon-borne in situ

30   measurements, Journal of atmospheric and oceanic technology, 27, 1652–1664, 2010.

Oncley, S. P., Friehe, C. A., Larue, J. C., Businger, J. A., Itsweire, E. C., and Chang, S. S.: Surface-layer fluxes, profiles, and turbulence measurements over uniform terrain under near-neutral conditions, J. Atmos. Sci., 53, 1029–1044, 1996.

Poggi, D. and Katul, G. G.: Flume experiments on intermittency and zero-crossing properties of canopy turbulence, Phys. Fluids, 21, 065103, 2009

35   Poggi, D. and Katul, G. G.: Evaluation of the Turbulent Kinetic Energy Dissipation Rate Inside Canopies by Zero- and Level-Crossing Density Methods, Boundary-Layer Meteorol., 136, 219–233, 2010

Pope, S. B.: *Turbulent flows*, Cambridge, 2000.

Rice, S. O.: Mathematical analysis of random noise, Bell. Syst. Tech. J., 24, 24–156, 1945.

Saddoughi, S. G. and Veeravalli, S. V.: Local isotropy in turbulent boundary layers at high Reynolds numbers, J. Fluid Mech., 268, 333–372, 1994.

Siebert, H., Lehmann, K., and Wendisch, M.: Observations of small-scale turbulence and energy dissipation rates in the cloudy boundary
5   layer, Journal of the atmospheric sciences, 63, 1451–1466, 2006.

Strauss L., Serafin S., Haimov S., and Grubišić V.:Turbulence in breaking mountain waves and atmospheric rotors estimated from airborne in situ and Doppler radar measurements. Q. J. R. Meteorol Soc., 141, 3207–3225, 2015

Sreenivasan, K., Prabhu, A. and Narasimha, R.: Zero-crossings in turbulent signals, Journal of Fluid Mechanics, 137, 251–272, 1983.

Wendisch M., and Brenguier, J-L., (eds): Airborne Measurements for Environmental Research: Methods and Instruments, Wiley-VCH Verlag
10   GmbH & Co. KGaA, 641p., 2013.

Wilson, D. J.: Concentration Fluctuations and Averaging Time in Vapor Clouds, American Institute of Chemical Engineers, New York, 1995.

Yee E., Kosteniuk, P. R., Chandler G. M., Biltoft, C. A. and Bowers J. F.: Measurements of level-crossing statistics of concentration fluctuations in plumes dispersing in the atmospheric surface layer, Boundary-Layer Meteorol., 73, 53–90, 1995.